

Changing concentration, lifetime and climate forcing of atmospheric methane

By JOS LELIEVELD^{1*}, PAUL J. CRUTZEN² and FRANK J. DENTENER¹ ¹*Institute for Marine and Atmospheric Research Utrecht, Princetonplein 5, 3584 CC Utrecht, The Netherlands,* ²*Max-Planck-Institute for Chemistry, P. O. Box 3060, D-55020 Mainz, Germany*

(Manuscript received 8 April 1997; in final form 4 September 1997)

ABSTRACT

Previous studies on ice core analyses and recent in situ measurements have shown that CH₄ has increased from about 0.75 to 1.73 μmol/mol during the past 150 years. Here, we review sources and sink estimates and we present global 3D model calculations, showing that the main features of the global CH₄ distribution are well represented. The model has been used to derive the total CH₄ emission source, being about 600 Tg yr⁻¹. Based on published results of isotope measurements the total contribution of fossil fuel related CH₄ emissions has been estimated to be about 110 Tg yr⁻¹. However, the individual coal, natural gas and oil associated CH₄ emissions can not be accurately quantified. In particular natural gas and oil associated emissions remain speculative. Since the total anthropogenic CH₄ source is about 410 Tg yr⁻¹ (~70% of the total source) and the mean recent atmospheric CH₄ increase is ~20 Tg yr⁻¹ an anthropogenic source reduction of 5% could stabilize the atmospheric CH₄ level. We have calculated the indirect chemical effects of increasing CH₄ on climate forcing on the basis of global 3D chemistry-transport and radiative transfer calculations. These indicate an enhancement of the direct radiative effect by about 30%, in agreement with previous work. The contribution of CH₄ (direct and indirect effects) to climate forcing during the past 150 years is 0.57 W m⁻² (direct 0.44 W m⁻², indirect 0.13 W m⁻²). This is about 35% of the climate forcing by CO₂ (1.6 W m⁻²) and about 22% of the forcing by all long-lived greenhouse gases (2.6 W m⁻²). Scenario calculations (IPCC-IS92a) indicate that the CH₄ lifetime in the atmosphere increased by about 25–30% during the past 150 years to a current value of 7.9 years. Future lifetime changes are expected to be much smaller, about 6%, mostly due to the expected increase of tropospheric O₃ (→OH) in the tropics. The global mean concentration of CH₄ may increase to about 2.55 μmol/mol, its lifetime is expected to increase to 8.4 years in the year 2050. Further, we have calculated a CH₄ global warming potential (GWP) of 21 (kgCH₄/kgCO₂) over a time horizon of 100 years, in agreement with IPCC (1996). Scenario calculations indicate that the importance of the climate forcing by CH₄ (including indirect effects) relative to that of CO₂ will decrease in future; currently this is about 35%, while this is expected to decrease to about 15% in the year 2050.

1. Introduction

Atmospheric methane (CH₄) is a moderately reactive trace gas with a lifetime** in the atmo-

sphere of about 7.9 years (Table 1). Most CH₄ is removed from the atmosphere through oxidation by hydroxyl radicals (OH) in the troposphere (Levy, 1971). Further, a fraction of about 7–11% is destroyed in the stratosphere and 1–10% is removed by bacterial consumption in soils (Born et al., 1990). The current global mean atmospheric CH₄ level (year 1995) is about 1.73 μmol/mol (i.e., μmol CH₄/mol air). During the last glacial maximum (~18,000 years BP) the CH₄ level was about 0.35 μmol/mol; it increased to about

* Corresponding author.

** The CH₄ “lifetime” (or turnover time) is defined as the total atmospheric CH₄ burden divided by the sum of all loss processes; the “adjustment” time (or response time) quantifies the decay of an instantaneous CH₄ emission pulse (Subsection 4.4).

Table 1. Atmospheric mixing ratios of CO₂, CH₄, N₂O, CFC-11 and CFC-12 during the last glacial, the pre-industrial period and from 1900–1995 (IPCC, 1990–1996; Montzka et al., 1996; Cunnold et al., 1997)

	CO ₂ μmol/mol	CH ₄ μmol/mol	N ₂ O nmol/mol	CFC-11 pmol/mol	CFC-12 pmol/mol
Last glacial (≈ 18000 yr BP)	195	0.35	244	0	0
1850	280	0.75	260	0	0
1900	296	0.97	292	0	0
1960	316	1.27	296	18	30
1970	325	1.42	299	70	121
1980	337	1.57	303	158	273
1990	354	1.72	310	258	484
1995	360	1.73	312	258	532
1995 annual increase	1.6 (0.45%)	0.008 (0.45%)	0.5 (0.25%)	−0.6 (−0.2%)	0
Present atmospheric lifetime (years)	50–200	7.9	120	50	102

0.75 μmol/mol by the middle of the 19th century (Rasmussen and Khalil, 1984; Chappellaz et al., 1990). Since then CH₄ increased much more rapidly as a result of agricultural expansion and industrialization, i.e., by more than 100% (Etheridge et al., 1992). Table 1 gives a summary based on recent studies and our own calculations as presented in section 4; also shown are the 1995 growth rates and the atmospheric lifetimes.

Atmospheric CH₄ growth rates were particularly fast during the 1970s, ~20 nmol/mol yr⁻¹ (Blake and Rowland, 1988), while they remained high during the 1980s, ~12 nmol/mol yr⁻¹. By the end of the 1980s and early 1990s, the CH₄ increase reduced to ~9 nmol/mol yr⁻¹, whereas in 1992 it was only very small, practically zero in the northern hemisphere (Dlugokencky et al., 1994a,b). During the past few years, the CH₄ growth rate approximately regained the value of 1991, ~8 nmol/mol yr⁻¹. Explanations for these rather strong fluctuations in the CH₄ trend are still ambiguous and will be further discussed in sections 3 and 4.

There is little doubt that the doubling of atmospheric CH₄ during the past 1–2 centuries is the result of anthropogenic emissions (Etheridge et al., 1992). Natural CH₄ sources constitute only about one third of the total present-day source (EPA, 1993). It mostly involves microbiological decay of organic matter under anoxic conditions in wetlands, in particular swamps, marshes and tundras. Important man-made sources are domestic ruminants,

rice fields, bacterial decay of wastes and sewage, and methane losses from fossil fuel use. It should be emphasized that the assessment of individual source strengths is very difficult, and is associated with uncertainties up to a factor of 2. The “scaling” problem intrinsic to extrapolation from local measurements is hard to deal with. For example, a large number of geographically specific soil properties affect both microbiological CH₄ production and destruction.

Global three-dimensional (3D) models can be used to assess the total source strength by calculating the CH₄ destruction by OH and evaluating the accuracy of OH calculations by methyl chloroform (CH₃CCl₃) simulations (Prinn et al., 1995). In Section 2 we describe a global model used to perform such an assessment, and in Section 3 we present the results from a global OH-CH₄ simulation and a more detailed discussion of emission estimates. Since emissions of CH₄ and of other reactive trace gases affect the abundance of OH, we have performed a 200 year (1850–1992–2050) scenario simulation to study CH₄ lifetime changes and associated indirect chemical effects. The scenario is presented in Section 2 and the calculations of the consequent CH₄ distributions and lifetimes in Section 4.

In the current atmosphere, one added CH₄ molecule absorbs infrared radiation (IR) about 25 times more efficiently than one added CO₂ molecule (Lelieveld et al., 1993). The main reason for this is that CO₂ levels are about 200 times higher,

so that many of its absorption lines are already saturated. The climate effects of increasing greenhouse gases are quantified in terms of their radiative forcing, i.e., their perturbation of the global mean radiation balance in W m^{-2} (IPCC, 1990). According to IPCC (1996) the total radiative forcing by increasing levels of CO_2 , CH_4 , N_2O and halocarbons during the past 150 years is about 2.5 W m^{-2} , of which 1.6 W m^{-2} is due to CO_2 and 0.47 W m^{-2} to CH_4 . Section 5 presents calculations which are in close agreement with this. Note that this 2.5 W m^{-2} only accounts for the direct forcing by well-mixed greenhouse gases, and it has an uncertainty of about 15%. Stratospheric ozone depletion and increased aerosol concentrations cause a negative (cooling) forcing of $1\text{--}2 \text{ W m}^{-2}$, however, this number is rather uncertain (IPCC, 1996). Although the estimated negative forcing by aerosols is expressed as a global average, it is largely restricted to the regions downwind of the emissions, so that this regional negative forcing cannot simply be discounted with the global effect of well-mixed greenhouse gases (IPCC, 1994).

Further, the increases of CH_4 and other chemically reactive gases, in particular carbon monoxide and nitrogen oxides, have led to an increase of tropospheric ozone, which enhances the greenhouse forcing by $0.2\text{--}0.6 \text{ W m}^{-2}$ (IPCC, 1996). The radiative forcing by tropospheric O_3 is of regional nature, largely spatially coinciding with that of pollution aerosols (but opposite in sign). In Section 5 we present an update of the radiative forcing of CH_4 and its indirect effects, e.g., through tropospheric O_3 . We also evaluate the CH_4 climate index, expressed as a Global Warming Potential, a measure of the time integrated CH_4 radiative forcing relative to that of CO_2 . Section 6 presents the conclusions.

2. Model description and emission scenario

The global 3D chemistry-transport model used in this study simulates the transport and chemistry of trace constituents in the troposphere (Crutzen and Zimmerman, 1991). The model has a Eulerian grid with 10 layers in the vertical dimension, accounting for atmospheric pressure levels from 1000–100 hPa (up to $\sim 16 \text{ km}$ altitude); the horizontal resolution is $10^\circ \times 10^\circ$ latitude by longitude.

Mass-conserving transport is driven by 3D wind fields obtained from meteorological observations over a ten year period (Oort, 1983). It may be argued that the meteorology during this decade does not ideally represent the two-century period covered by this study. Thus temperature, humidity, cloudiness etc. are the same for the three emission scenarios considered (1850, 1992, 2050). Nonetheless, we claim that the 2-, 3- or more-fold increases of reactive trace gas emissions since pre-industrial times dominate atmospheric chemical compositions rather than climate changes.

The large-scale diffusion coefficients are proportional to the day-to-day variances and covariances of the monthly wind fields. Vertical transport of short-lived trace species in precipitating deep convective clouds has been parameterized with a mass-flux scheme, based on statistics of convective precipitation (Feichter and Crutzen, 1990). The tropospheric chemistry description in the model accounts for $\text{CH}_4\text{-CO-NO}_x\text{-O}_3\text{-OH}$ photochemistry, pertaining to the background global troposphere (Crutzen and Zimmermann, 1991). Heterogeneous processes have also been accounted for to simulate the chemical effects by aerosols and clouds (Dentener and Crutzen, 1993). Tracer studies of the chlorofluorocarbons CFC-11 and CFC-12 (Zimmermann, 1987), radioactive ^{85}Kr (Zimmermann et al., 1989), ^{222}Rn (Feichter and Crutzen, 1990) and CH_3CCl_3 (Crutzen and Zimmermann, 1991; Dentener, 1993) have been performed to test the model performance. It appears that especially the relatively long-lived trace species are well represented by the model.

The CH_4 emission distributions for wetlands and rice paddies have been adopted from Aselman and Crutzen (1989), and that of animals from Crutzen et al. (1986). Total emission source strengths are given in Table 2. Methane emissions by termites are distributed according to Fung et al. (1991). Industrial emissions have been scaled to those of CO_2 (Marland and Rotty, 1984; WRI, 1990; Lelieveld and Van Dorland, 1995). Biomass burning emissions were adopted from Hao et al. (1991). Fossil fuel related CH_4 emissions have been based on the compilation discussed in EPA (1993). For descriptions of deposition routines and the emission distributions of other trace species we refer to Crutzen and Zimmermann (1991), Lelieveld et al. (1993) and Lelieveld and Van Dorland (1995).

Table 2. *Estimated pre-industrial, contemporary and future emissions, updated after the IS92a scenario of IPCC (1992) (in Tg yr⁻¹; NO_x in Tg N yr⁻¹)*

Emission source	1850			1992			2050		
	CH ₄	CO	NO _x	CH ₄	CO	NO _x	CH ₄	CO	NO _x
energy use				110	540	25	175	760	54
biomass burning	10	110	2	40	400	6	50	550	7.5
vegetation		100			100			100	
CH ₄ oxidation ^a		345			845			1330	
natural NMHC		325			325			325	
anthropogenic NMHC		30			120			165	
wildfires		30			30			30	
soils			5			5			5
lightning			5			5			5
domestic ruminants	20			80			165		
wild ruminants	5			5			5		
rice paddies	27			80			95		
animal wastes	5			30			60		
landfills	10			40			75		
wastewater	6			25			45		
wetlands	145			145			145		
oceans	10	40		10	40		10	40	
freshwaters	5			5			5		
termites	20			20			20		
CH ₄ hydrates	5			10			15		
total	268	980	12	600	2400	41	865	3300	71.5

^a Not included in the model as emission but calculated as a chemical source in the troposphere.

It is likely that desiccation of peat bogs and wetland conversion for agricultural purposes (e.g., rice production) have decreased the areal extent of natural wetland CH₄ emissions during the past 150 years. On the other hand, since methanogenic bacteria are sensitive to temperature (Cicerone and Oremland, 1988), global warming may stimulate CH₄ production in wetlands and increase the thaw season in high latitudes. We have, rather arbitrarily, assumed that these natural emissions have remained constant over the 200 year period considered. Because the world human population has increased by a factor of 4 during the past 150 years, we hypothesize that the anthropogenic emissions through biomass burning and domestic ruminants were about 75% less in 1850.

Studies of rice cultivation indicate that the paddy area harvested by the middle of the past century was up to one third of the current area (Darmstadter et al., 1987; Aselmann and Crutzen, 1989), so that we have reduced the pre-industrial emissions from this source accordingly. Furthermore, we have assumed that the CH₄

releases from wastes and sewage were only 15 Tg yr⁻¹ and that emissions from energy use can be neglected in the simulations of the mid 1800s.

The future (2050) emission trend estimates (Table 2) are based on the IS92a scenario developed by the Intergovernmental Panel on Climate Change (IPCC, 1992), including some modifications based on recent developments (IPCC, 1996). It accounts for World Bank and United Nations population forecasts, and deforestation rate and agricultural development studies by the Food and Agriculture Organization. General assumptions basic to the IS92a scenario are that the world population in 2050 is 9.1×10^9 and that the average annual economic growth is 2.4%. The assumption involving fossil fuel related emissions include a global increase in energy use efficiency (per unit of gross national product) of 0.8% yr⁻¹ in the period to 2025, and 1% yr⁻¹ from 2025 to 2050 (IPCC, 1992). It has been anticipated that towards the second half of the next century limitations in fossil fuel resources start playing a role; advances in energy technolo-

gies may also be expected. Needless to say that these developments can strongly influence trace gas emissions. Assumptions based on available oil and gas reserves have been adopted from the study of Masters et al. (1991).

The radiative forcing calculations have been performed with a code originally developed by Morcrette (1991), which treats 2 short-wave and 6 long-wave spectral intervals, and it has been extended to account for non-CO₂ greenhouse gases and aerosols. The model has been compared with five different radiation schemes in the context of an Ozone Forcing Intercomparison (Shine et al., 1995). The forcing calculations use the Fixed Dynamical Heating formulation (Mode B in WMO, 1992). This deviates from the instantaneous radiative forcing calculation in which the net radiative flux change at the tropopause is calculated keeping all other parameters (e.g., H₂O and temperature) constant in troposphere and stratosphere. In our results the stratospheric temperatures have been allowed to adjust to a new equilibrium in the radiation model, making use of the fact that this new equilibrium is reached within a few months after applying the perturbation. Note that this adjustment in the troposphere takes up to decades because of the large heat capacity of the oceans. More details and recent updates of the radiation scheme are described in Van Dorland et al. (1997).

3. Sources of methane

3.1. Total CH₄ source

About 90% of the removal of CH₄ from the atmosphere occurs through reaction with OH, mostly in the troposphere. Although concentrations of OH are highly variable in space and time, its global mean distribution can be relatively accurately determined from model calculations. We have tested our model calculated OH by simulating methylchloroform (CH₃CCl₃) concentrations based on known emissions, and by comparing the results against measurements from the ALE/GAGE global network (Prinn et al., 1995). This compound has been used as a solvent and cleaning agent, and its release to the atmosphere is well quantified. For example, the recent emission reduction, as reported by the industry, is consistent with the observed atmospheric CH₃CCl₃ decrease

(Montzka et al., 1996). Apart from a small sink by dissolution in the oceans (6%) and photolysis in the stratosphere (3%), CH₃CCl₃ is destroyed in the atmosphere by its reaction with OH.

We obtain quite good agreement between our model results and measured CH₃CCl₃, although the model CH₃CCl₃ is slightly lower (Fig. 1). Nevertheless, this indicates that the main features of the global OH distribution are simulated within about 10%. In turn, this provides confidence that the total CH₄ destruction in the troposphere, 510 Tg yr⁻¹, is calculated adequately, although the slight underestimation of OH may indicate that this value is a lower limit. By also accounting for loss processes in soils and the stratosphere, and the measured annual increase, we derive a total CH₄ sink of 600 ± 80 Tg yr⁻¹, which must equal the total source (Table 3). IPCC (1996) mentions a 20 Tg lower annual CH₄ destruction by tropospheric OH of 490 Tg yr⁻¹. Nevertheless, the IPCC (1996) implied total source (597 Tg yr⁻¹) is in good agreement with our estimate.

This CH₄ source estimate is also within the range of 520–625 Tg yr⁻¹ calculated by Hein et al. (1997) who applied an inverse modelling technique, referring to the year 1987, to deduce methane sources from observed temporal and spatial variations of atmospheric CH₄ mixing ratios. A global 3D model was used and OH fields were validated on the basis of CH₃CCl₃ simulations. Inverse modelling involves iterative optimization of the agreement between model calculated and measured CH₄ from a global network, including ¹³CH₄/¹²CH₄ isotope ratios (Fung et al., 1991; Quay et al., 1991). Hein et al. (1997) concluded that emission estimates of rice paddies, wetlands, landfills, oil associated gas and natural gas leakage have relatively large uncertainty ranges, up to

Table 3. *Estimated sinks (and implied total source) of atmospheric methane*

Sinks	Tg yr ⁻¹
reaction with OH in the troposphere	510 ± 50
bacterial oxidation in soils	30 ± 15
reactions with OH, Cl and O(¹ D) in the stratosphere	40 ± 10
atmospheric increase	20 ± 5
total sink plus increase (=source)	600 ± 80

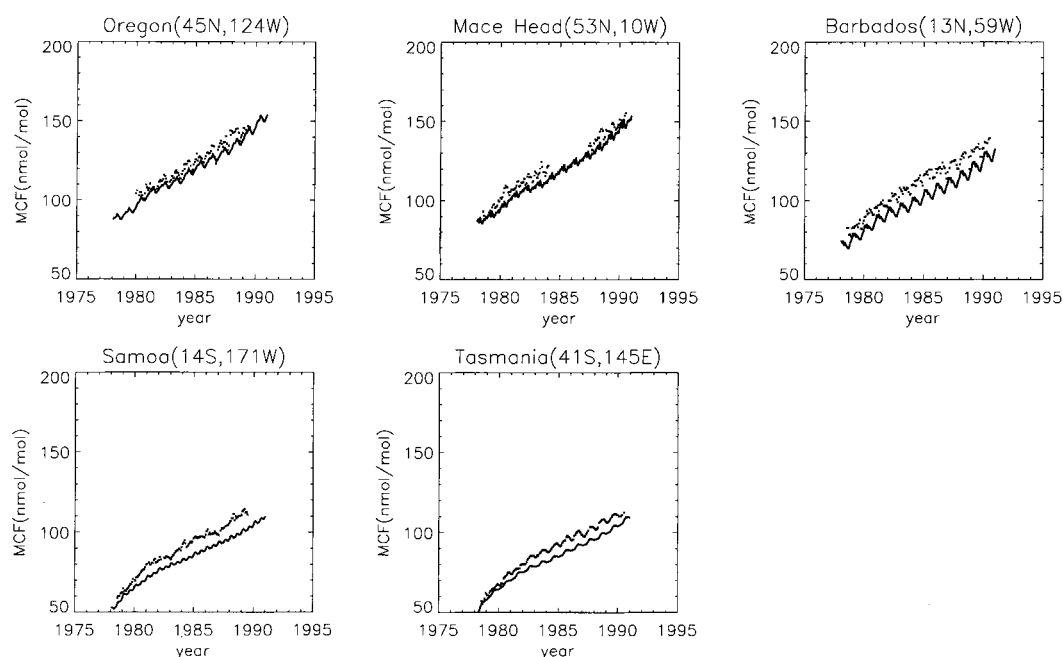


Fig. 1. Model calculated CH_3CCl_3 concentrations (solid lines), compared with observations (dotted) from Prinn et al. (1995).

about $\pm 50\%$. On the other hand, methane emissions from coal mines and domestic ruminants appear to be somewhat better constrained, within about $\pm 25\%$. Individual source estimates will be further discussed in Subsections 3.3 to 3.6.

3.2. Total fossil CH_4 source

Biogenic methane in the natural atmosphere reflects the $^{14}\text{C}/^{12}\text{C}$ ratio in atmospheric CO_2 , determined by $^{14}\text{CO}_2$ production by cosmic radiation. The $^{14}\text{CO}_2$ is taken up by vegetations and takes part in the CO_2/CH_4 cycle, i.e., assimilation and methanogenesis of organic material. The fraction of ^{14}C in the increasing amount of CH_4 in the atmosphere is sensitive to fossil fuel related CH_4 emissions because "old" methane from geological deposits is depleted in ^{14}C . By inference, the relative contribution from fossil fuel related CH_4 sources can be estimated from $^{14}\text{CH}_4/^{12}\text{CH}_4$ measurements in the atmosphere. Wahlen et al. (1989) calculated that $21 \pm 3\%$ of all atmospheric CH_4 is old methane. An even higher fraction, up to 30%, was estimated by Lowe et al. (1988). However,

Quay et al. (1991) estimated 16%, while Manning et al. (1990) obtained a fractional contribution of about 25%.

Overall we adopt a fraction of 20%, which seems to be generally accepted, with an uncertainty range of $\pm 4\%$. Thus with a total source strength of $600 \pm 80 \text{ Tg yr}^{-1}$ (Table 3), it can be argued that "old" methane contributes about 85–160 Tg yr^{-1} to CH_4 emissions. A small fraction, 5–15 Tg yr^{-1} , is attributed to methane volatilization from warming permafrost regions, loss of CH_4 hydrates from ocean sediments and other minor geological CH_4 sources (EPA, 1993). Hence, we obtain a "best estimate" of $110 \pm 45 \text{ Tg yr}^{-1}$ associated with the mining and use of fossil fuels (Table 4). We emphasize that the indirectly derived best estimate of the total fossil CH_4 source has a smaller uncertainty compared to those of individual fossil sources, as will be discussed in Subsection 3.5. It should be noted that IPCC (1996) also assumes a 20% fossil fuel contribution to the total CH_4 source, which would be 120 Tg yr^{-1} of 597 Tg yr^{-1} . However, the IPCC (1996) listing of source estimates (Table 2.3b) mentions

Table 4. *Estimated fossil fuel related and other $^{14}\text{CH}_4$ -free emissions*

Sources	Tg yr ⁻¹
coal mining and combustion	45 ± 15
oil and gas related emissions	65 ± 30
total fossil fuel related	110 ± 45
methane hydrates and other geological sources	10 ± 5
total $^{14}\text{CH}_4$ -free (20 ± 4% of 600 ± 80 Tg yr ⁻¹)	120 ± 40

only 100 Tg yr⁻¹ for fossil fuel related CH₄ releases. Nevertheless, it can be argued that these estimates are within the limits of uncertainty.

3.3. Natural sources

The adding of current natural and man-made source estimates and associated uncertainties provides a relatively inexact method to estimate the total CH₄ source, yielding roughly 300–800 Tg yr⁻¹. Estimates of natural CH₄ emissions have large uncertainties, for example, wetlands may contribute 70–175 Tg yr⁻¹ (EPA, 1993). However, in Subsection 4.3, we present model simulations of pre-industrial CH₄ levels and compare these with ice core data, which constrains this source to about 115–175 Tg yr⁻¹ (Table 5). Although tropical wetlands occupy less than 20% of the global wetland area, they cause about 60% of the emissions, mostly due to the relatively high soil temperatures, high plant production and intense solar radiation at low latitudes (Bartlett and Harriss, 1993). The majority of non-tropical wetland CH₄

Table 5. *Estimated natural methane emissions*

Sources	Tg yr ⁻¹
wetlands	145 ± 30
termites	20 ± 20
oceans	10 ± 5
wild ruminants	5 ± 5
freshwaters	5 ± 5
CH ₄ from sediments ^a	5 ± 5
total natural	190 ± 70

^a We assume that half the “old” CH₄ release of 10 Tg yr⁻¹ is from melting permafrost regions caused by anthropogenic climate warming, while the other half is natural, e.g., from hydrate destabilization.

emissions originates from boreal wetlands, e.g., in northern Canada and Siberia. Arctic tundras emit comparatively little because of the short duration of the thaw season. Temperate wetlands are less important since they occupy less than 5% of the global wetland area. A main source of uncertainties in wetland emission estimates is the poor characterization of nutrient and flooding conditions. Moreover, it is difficult to quantify the relative contribution of bacterial CH₄ consumption (methylotrophy) during its diffusion from the anoxic production (methanogenesis) zone to the surface (Reeburgh et al., 1994). Another natural source of methane is release by termites. Emissions from termite nests vary strongly, up to a factor of 100, largely related to the size of the colonies. Hence global source estimates are uncertain, about 10–40 Tg yr⁻¹, with a central value of 20 Tg yr⁻¹ (IPCC, 1992; Martius et al., 1993). Natural CH₄ sources include the destabilization of gas hydrates and the melting of permafrost. Although large amounts of methane are stored as hydrates in marine and continental sediments, only a very small fraction leaks to the atmosphere. Finally, emissions from oceans and freshwaters are estimated to be 5–25 Tg yr⁻¹.

3.4. Agricultural sources

Biogenic CH₄ emissions of agricultural origin include livestock and rice cultivation. Microorganisms in the forestomach (rumen) of domestic ruminants, in particular of cattle, produce methane in appreciable amounts. The methane is released by exhalation or eructation. The amount of CH₄ produced through enteric fermentation primarily depends on the feed intake. Typically, the average emission factors are relatively low in southern Asia (~28 kg yr⁻¹ per animal) and high in western Europe (~64 kg yr⁻¹) (Crutzen et al., 1986; EPA, 1994). Most of the CH₄ release by animals is produced by ruminant cattle (Table 6); other domestic and wild animals add about 25 Tg yr⁻¹. Domestic ruminants are estimated to contribute 80 ± 20 Tg CH₄ yr⁻¹, while wild animals release ~5 Tg yr⁻¹ (Tables 5, 6). In addition, anaerobic decomposition of animal wastes may contribute 30 ± 15 Tg yr⁻¹ (EPA, 1994; Berges and Crutzen, 1996).

About half of all CH₄ emissions occurs in the tropics. A significant part of these are from rice

Table 6. *Estimated agricultural methane emissions*

Sources	Tg yr ⁻¹
biomass burning	40 ± 30
domestic ruminants	80 ± 20
animal wastes	30 ± 15
rice paddies	80 ± 50
total agricultural	230 ± 115

cultivation, mostly from southern Asia. Emissions from rice paddies depend on many local factors, in particular temperature, soil type, microbiology, rice variety, fertilization practices and flooding conditions. In particular temperature and the flooding regime appear to be important. For example, rainfed rice fields emit less CH₄ compared to irrigated paddies due to periodic droughts during the growth season (Neue and Sass, 1994). Since floodings and soil factors are not well known, estimates of global rice paddy CH₄ emissions are rather uncertain. IPCC (1992) mentions a range of 20–150 Tg yr⁻¹ and WMO (1994) of 20–100 Tg yr⁻¹, however, the lower limit of these ranges appears inconsistent with sensitivity calculations with our global model. In fact, the strong increase of global rice cultivation during the past century probably has contributed significantly to the observed CH₄ increase. In recent decades, the areal growth of rice fields may have been small, although the crop yields have increased substantially.

Savanna burning, deforestation, shifting cultivation, and firewood and agricultural waste burning are also important sources of CH₄ (Crutzen and Andreae, 1990; Andreae and Warneck, 1994). In addition, the burning of agricultural residues, e.g., of rice straw, sugarcane and other agricultural disposals, is also significant. However, the estimates of CH₄ emissions from biomass burning are rather uncertain, ranging from 10–70 Tg yr⁻¹. Main causes are the lack of information about the areal extents of the burning and the difficulty of quantifying the flaming and smoldering phases, associated with differences in combustion temperatures and efficiencies (Lobert et al., 1991).

3.5. Fossil fuel related sources

As mentioned earlier, the total CH₄ release related to the mining and use of fossil fuels is

110 ± 45 Tg yr⁻¹, however, individual sources are poorly quantified. The least uncertain of these is the use of coal, accounting for about 45 ± 15 Tg yr⁻¹ (Table 4). It should be emphasized that most coal associated emission studies have been performed in western Europe and the USA, which may not be representative for Asian coal mines, for which measurements are not available (Kirchgessner et al., 1993; EPA, 1994). Ventilation of underground mines for safety reasons contributes most. A minor fraction of the CH₄ is currently recovered from the mine gas for local energy production. Surface coals contain less methane compared to underground coals, so that emissions are much smaller. Most coal production and associated CH₄ releases occur in China, Russia and the USA. Additional important source regions are eastern Europe, South Africa and the UK. In fact, 90% of coal associated CH₄ emissions are caused by only 10 large coal producing countries (EPA, 1994).

By inference from the above mentioned estimates of the total fossil CH₄ source and the coal associated source, oil and gas related emissions may amount to 65 ± 30 Tg yr⁻¹, although the extremes of this range seem rather unlikely. A recent study carried out within the IEA Greenhouse Gas R&D Programme estimated the total methane release by oil and natural gas systems to be somewhat lower, about 47 (40–70) Tg yr⁻¹ (IEA, 1997). Oil and natural gas production in Russia and the USA account for more than 40% of the global energy production from these fuels (EPA, 1994). Reliable emission estimates are lacking since measurements of vents are close to absent, and measurements of gas leakages from transport and distribution are scarce. Oil associated gas is usually not used for energy production; it is vented, flared or re-injected into the oil field. The amounts released during oil production are substantial, whereas the fraction vented is unknown. Moreover, some methane may survive due to inefficient combustion during flaring. Aircraft measurements over Siberian production areas confirm the significance of oil associated gas emissions (Sugawara et al., 1996; Tohjima et al., 1996). Further, crude oil is usually stored for some time during which CH₄ can be outgassed.

Leakage of natural gas may occur during production, transmission, storage and distribution. Recently, much emphasis has been placed on CH₄

releases from Siberian gas fields, however, estimates are highly speculative (Andronova and Karol, 1993; Dlugokencky et al., 1994a). Only little information is available about the state of maintenance and gas releases from the pipeline network through Russia and the other former Soviet states, although large losses from high pressure pipelines seem unlikely (Zittel, 1997). Measurements of methane emissions from compressor stations and transmission pipelines in Russia have been conducted jointly by RAO Gazprom and Ruhrgas AG in 1997. The methane emissions from this sector have been estimated at less than 1% of the natural gas transported. The gas production sector in West-Siberia will be investigated by the end of 1997 (Ruhrgas, personal communication).

Natural gas losses in the USA mostly occur during transmission and storage, while production appears to be less important (Harrison and Cowgill, 1996; cited in Shorter et al., 1996). In the USA methane emissions from the natural gas industry have been estimated to be about 6 Tg yr⁻¹, i.e., 1.4% of the natural gas production in the reference year 1992 (transmission/storage 37%, production 27%, processing 12%, distribution 24%) (EPA, 1996). Low-pressure networks, e.g., in the USA, Germany and the Netherlands have losses that are usually less than a percent (Mitchell, 1993; Lamb et al., 1995; Shorter et al., 1996). Overall, the currently available information is insufficient to quantify these sources worldwide and distinguish natural gas from oil associated emissions in the global CH₄ budget.

3.6. Domestic waste and sewage

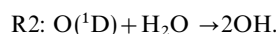
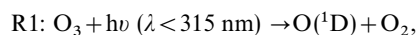
Microbiological decomposition of domestic waste and sewage produces substantial amounts of methane. In particular landfills provide conditions favourable for CH₄ formation, and the global source is estimated at 40 ± 20 Tg yr⁻¹; the USA is the largest source country with a fractional contribution of 40% or more (Bingemer and Crutzen, 1987; EPA, 1994). Main controlling factors are landfill moisture and acidity. Improved waste management, recycling and biogas recovery as well as incineration are cost-effective in reducing CH₄ emissions. The same is true for improved wastewater treatment. Note that reduction of these sources by technological methods and recycling

could very well contribute to the stabilization of atmospheric CH₄. More than 90% of all CH₄ release from sewage systems is of industrial origin; domestic sewage is thought to be of minor importance. Industrial waste water sources include food and paper industries and oil refineries. Current emissions from these sources are estimated at 25 ± 10 Tg yr⁻¹ (IPCC, 1992; EPA, 1994).

4. Methane distribution and lifetime

4.1. Chemical feedbacks

Methane removal from the atmosphere is largely a consequence of its reaction with OH, formed via the action of solar radiation on ozone and water vapour:



The reaction of hydroxyl with methane and other gases destroys OH, limiting its lifetime to a few seconds. On a global scale, about half of the OH is removed by emissions of carbon monoxide (CO) and most of the rest by methane and its reaction products (Law and Pyle, 1993; Crutzen, 1995). Although OH is rapidly destroyed, it is partly replenished as a by-product in the CH₄ and CO oxidation chains. Moreover, additional OH is formed when the oxidation occurs in the presence of nitrogen oxides (NO_x = NO + NO₂). Table 7 presents the main reaction sequence (see also Fig. 2). Next to OH formation, e.g., through reactions R1 and R2, the partitioning between HO₂ and OH by reaction R6 plays an important role in NO_x-rich air, thus enhancing OH. Further, the destruction of CH₄ yields formaldehyde (CH₂O)

Table 7. Main reaction sequence that leads to O₃ formation by CH₄ oxidation in an NO_x-rich environment. Note that further breakdown of CH₂O (R5) additionally yields O₃ and OH

R3: CH ₄ + OH (+ O ₂)	→ CH ₃ O ₂ + H ₂ O
R4: CH ₃ O ₂ + NO	→ CH ₃ O + NO ₂
R5: CH ₃ O + O ₂	→ CH ₂ O + HO ₂
R6: HO ₂ + NO	→ NO ₂ + OH
R7: 2NO ₂ + hν (λ < 420 nm)	→ 2NO + 2O
R8: 2O ₂ + 2O (+ M)	→ 2O ₃ (+ M)
net: CH ₄ + hν + 4O ₂	→ 2O ₃ + CH ₂ O + H ₂ O

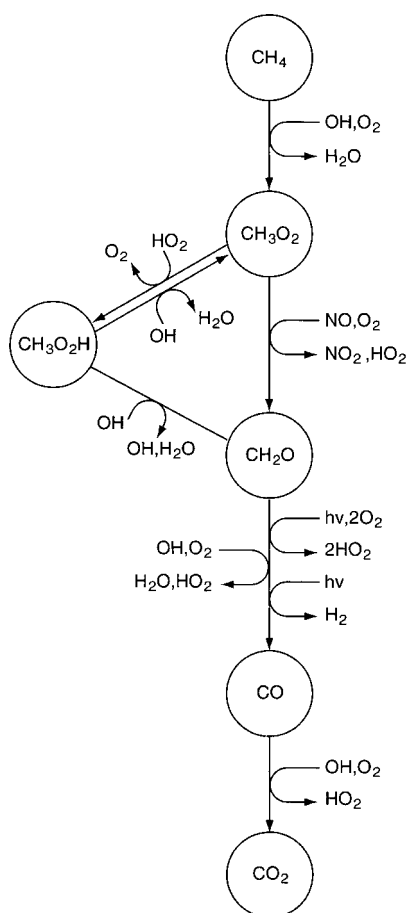


Fig. 2. Major reactions in the CH₄ oxidation chain. In NO_x-poor air CH₂O is mostly formed through CH₃O₂H (left), whereas in NO_x-rich air the direct path to CH₂O dominates.

which, in turn, photodissociates and reacts with OH to yield HO₂ radicals and carbon monoxide. Through this pathway CH₄ oxidation in the troposphere forms about 845 Tg CO yr⁻¹, which is about 35% of the total atmospheric CO source (Table 2). Anthropogenic sources (including anthropogenic CH₄ and other hydrocarbons) contribute about 65–70% to the total atmospheric CO burden of 400 Tg; this fraction is expected to increase to about 75% in the year 2050 (Table 2).

It should be emphasized that the above mentioned reaction paths (Table 7) assume the presence of nitrogen oxides. In the pristine pre-industrial atmosphere as well as the contemporary

remote marine atmosphere, NO_x levels are very low. The short NO_x lifetime of about 1–2 days limits its transport from the source regions. At these low NO_x levels (i.e., less than 25–50 pmol/mol) the hydroperoxy radicals produced in the breakdown of CH₄ and CO cannot react with NO but destroy O₃ and thus limit the regeneration of OH radicals.

Thus, if NO_x levels are relatively high, methane oxidation in the atmosphere is a net source of ozone and hydroxyl radicals, whereas net destruction of O₃ and OH prevails if NO_x is low. Further, about three quarters of the OH reacts with CO, of which 35% originates from CH₄ destruction. On a global scale, emissions of CO and CH₄ both remove about half of the OH. Evidently, CH₄ emissions and concurrent CO and NO_x emissions should be evaluated simultaneously, also because these species to a large extent have the same sources, i.e., biomass burning and fossil fuel related emissions. The chemical feedbacks of these gases on OH, and thus the lifetime of CH₄, depend critically on their source strengths and transports throughout the global atmosphere (Chameides et al., 1977; Isaksen and Hov, 1987). These considerations also indicate that in the pristine (NO_x-poor) atmosphere a relatively strong positive feedback exists between growing CH₄ emissions, loss of OH and a consequently increasing CH₄ lifetime. On the other hand, in more polluted environments (NO_x-rich) this feedback is reduced since OH losses are partly compensated by O₃ formation and OH regeneration. This aspect will be further addressed in Subsection 4.4.

4.2. Recent CH₄ trend change

The atmospheric growth rate of CH₄ was particularly large in the decades before the 1980s (Etheridge et al., 1992). It decreased by a factor of 2 by the end of the 1980s to about 9 nmol/mol yr⁻¹, roughly equal to the current CH₄ increase. However, during 1992 the upward CH₄ trend reached a temporary minimum. In fact, in the northern hemisphere methane increased only by 1–2 nmol/mol during this period, and the growth reduction was strongest between the equator and 30°N (Dlugokencky et al., 1994a). Globally, the sources must have decreased and/or the sinks must have increased by about 10 Tg yr⁻¹ in 1992 compared to the previous years. Evidently,

an explanation challenges our knowledge about the emissions and sink processes that control the levels of atmospheric methane. Next we discuss some possible causes.

The sudden CH₄ trend depression coincided with the eruption of Mt Pinatubo in the Philippines (15°N) in June 1991. This volcano deposited 15–20 Tg SO₂ into the stratosphere, which was converted into sulfate aerosol within several months. Although the sulfur species were initially released near 15°N, a considerable fraction reached the southern hemisphere, covering the 30°N to 20°S latitude band relatively rapidly (McCormick et al., 1995). Several months after the eruption a temporary stratospheric ozone reduction of about 6% occurred in the tropics, mostly due to aerosol induced warming of the stratosphere and consequent dynamical lifting (Labitzke and McCormick, 1992; Brasseur and Granier, 1992). Further, since sulfate aerosol provides a reactive surface to catalyze heterogeneous O₃ loss, anomalously strong depletion of the ozone layer took place in 1992 (Gleason et al., 1993). After about 2 years most of the aerosol was removed from the stratosphere by sedimentation.

Satellite observations of aerosol optical depth as well as Lidar and balloon sounding data showed that the Pinatubo aerosol loading of the stratosphere was a factor of 40–50 higher compared to the pre-Pinatubo situation. This caused a mean surface temperature decrease in the northern hemisphere of 0.5–1 K and a global average decrease of about 0.5 K (Dutton and Christy, 1992). The largest Pinatubo aerosol induced surface cooling, derived both from observations and from climate modelling, occurred in 1992, reaching a maximum over the northern hemispheric continents during late summer and fall of that year (Lacis and Mishchenko, 1995; Robock and Mao, 1995).

Temperature is one of the most sensitive factors of methanogenesis in anaerobic ecosystems (Harriss and Frolking, 1992; Westermann, 1993). Dlugokencky et al. (1994a) estimated that the 1992 temperature effect of Pinatubo aerosol reduced the wetland CH₄ emissions by about 2 Tg, based on a temperature dependence of high latitude wetlands and bogs (Fung et al., 1991). However, the aerosol effect was also significant in the tropics and subtropics in the northern hemisphere, where considerable wetland CH₄ emissions

occur (Bartlett and Harriss, 1993; Hogan and Harriss, 1994). Rice field CH₄ emissions are also strongly temperature dependent (Neue and Sass, 1994). Methanogenic bacteria are most sensitive to temperature variations under sub-optimal conditions, i.e., 20–30°C. This temperature range is typical for the latitudes where rice fields are located. For example, Holzapfel-Pschorn and Seiler (1986) observed an emission doubling from a 20 to 25°C soil temperature increase. Parashar et al. (1993) even measured an emission doubling from a temperature change of only 25 to 27°C.

An additional sensitive factor in wetland and rice field CH₄ emissions is the water table (Whalen and Reeburgh, 1992; Neue and Sass, 1994). The methane is produced in the flooded anoxic zone after which it is partly destroyed during upward diffusion through the oxic zone. Soil drying enhances bacterial CH₄ oxidation and reduces its release to the atmosphere. As a consequence of the continental Pinatubo cooling the summertime land-ocean temperature contrasts and the monsoon intensity may have been reduced in 1992. Thus, a decrease of the summer monsoon precipitation in subtropical latitudes may have contributed to a lowering of the water table and suppression of CH₄ emissions. Unfortunately, accurate precipitation data are lacking to provide empirical support. Nevertheless, most rice field emissions occur in northern low latitudes, where the 1992 CH₄ growth deceleration was strongest. Overall, the Pinatubo temperature and consequent hydrological effects on CH₄ emissions were probably substantial. It should be mentioned that also CH₄ breakdown by its reaction with OH is temperature dependent, and that a temperature decrease leads to reduced evaporation and OH formation through reaction R2. However, the effect from a 0.5 K temperature change on OH is relatively small.

Furthermore, the temporary acceleration of stratospheric ozone loss in 1992 has caused an increase of ultraviolet (UV) radiation penetration into the troposphere. It has been hypothesized that this has enhanced OH formation and thus CH₄ destruction (Madronich and Granier, 1992; Bekki et al., 1994; Fuglestvedt et al., 1994). We used our global 3-D model to perform a sensitivity calculation, by decreasing stratospheric O₃ columns according to satellite observations (TOMS) between 1980 and 1990 (ΔO_3 during this period

was -3 to -6% , mostly in middle and high latitudes). The largest stratospheric O_3 reduction occurred at high latitudes during spring. The results indicate tropospheric OH enhancements by 1 to 5% at middle to high latitudes, respectively, and a global mean increase of 0.5–1%. This causes a CH_4 trend reduction of approximately 3–4 Tg per decade (~ 0.1 nmol/mol yr $^{-1}$). This effect, although in the right direction, is too small to account for the observed CH_4 growth reduction since the 1970s. Nevertheless, the additional O_3 loss that occurred due to the Pinatubo aerosols has enhanced this effect, accounting for part of the 1992 CH_4 trend depression. Dlugokencky et al. (1996) noted that, initially, scattering from the Pinatubo aerosols and UV absorption by SO_2 have decreased the UV flux during late-1991 and early-1992, thus moderating the consequent OH effect on CH_4 .

Thus, we propose that the Pinatubo temperature and hydrological effects have played an important role in the 1992 CH_4 trend depression. This is consistent with the observation that the strongest reduction occurred in the northern tropics and subtropics. Furthermore, Lowe et al. (1994) indicated that a decrease of southern hemispheric biomass burning CH_4 emissions may have played an additional role. It is likely that this also contributed to a global decrease of CO emissions (Granier et al., 1996). Reduction of CO by about 6% per year between 1990 and 1993 (Novelli et al., 1994) and consequently increasing OH levels enhance CH_4 destruction, which should be particularly significant in low latitudes. Table 8 summarizes these possible causes for the CH_4 trend depression in 1992, assuming that they each contributed roughly 2 ± 2 Tg yr $^{-1}$. In fact, it seems likely that

Table 8. *Likely causes of the 1992 CH_4 trend depression*

Main cause (total ~ 10 Tg CH_4 yr $^{-1}$)
surface temperature decrease (Pinatubo)
reduced wetland emissions
reduced rice field emissions
reduced monsoon intensity (Pinatubo)
lowering water table, enhancing soil CH_4 oxidation
increased UV flux and OH formation (Pinatubo)
reduced biomass burning CH_4 emissions
reduced biomass burning and industrial CO emissions
reduced CO + OH, increased OH

this combination of factors explains the 1992 trend break.

Finally, Dlugokencky et al. (1994a) suggested that Russian fossil fuel related CH_4 emissions decreased substantially during 1992. In particular oil associated CH_4 emissions from the Tyumen production field in Siberia may have decreased during the past decade (Plotnikov et al., 1995). However, this is unlikely to be very important for 1992 since it is not consistent with the CH_4 trend recovery after 1992.

4.3. Simulated CH_4 distributions

The simulated contemporary CH_4 distribution (Fig. 3) corresponds well to that derived from the NOAA/CMDL network (Steele et al., 1987,1992; Dlugokencky et al., 1994b). Discrepancies are at most a few %, close to the measurement uncertainty of about 1% (Dlugokencky et al., 1994b). The calculated difference between northernmost and southernmost NOAA/CMDL sampling sites, i.e., comparing Antarctica to Greenland and northern Canada (~ 150 nmol/mol), agrees with the observations (Fig. 3). Mean CH_4 levels in the northern hemisphere are 5–6% higher than in the southern hemisphere, owing to the 3 times larger source strength in northern latitudes. Longitudinal variations are relatively strong in the northern hemisphere, being most pronounced at about 50° north (up to ~ 0.1 μ mol/mol). Such variations are small in the southern hemisphere and basically absent in high latitudes, as sources in these regions are small.

Longitudinal CH_4 variations are considerably smaller in the free troposphere compared to the boundary layer. Seasonal CH_4 variations (not shown) amount to $\sim 2\%$ in the southern and up to $\sim 4\%$ in the northern hemisphere; concentrations reach a maximum during winter. Despite the high latitude wetland emissions during the thaw season, the coincident summertime OH maximum suppresses CH_4 levels during this season. Latitudinal gradients are strongest across the Intertropical Convergence Zone (ITCZ), as inter-hemispheric exchange is relatively slow (~ 1 year). At the 0° meridian this tropical gradient reaches 0.5 nmol/mol per degree latitude. Note that this gradient at 0° is particularly strong during northern winter, whereas a similarly strong gradient occurs along 80°E (over India) during summer,

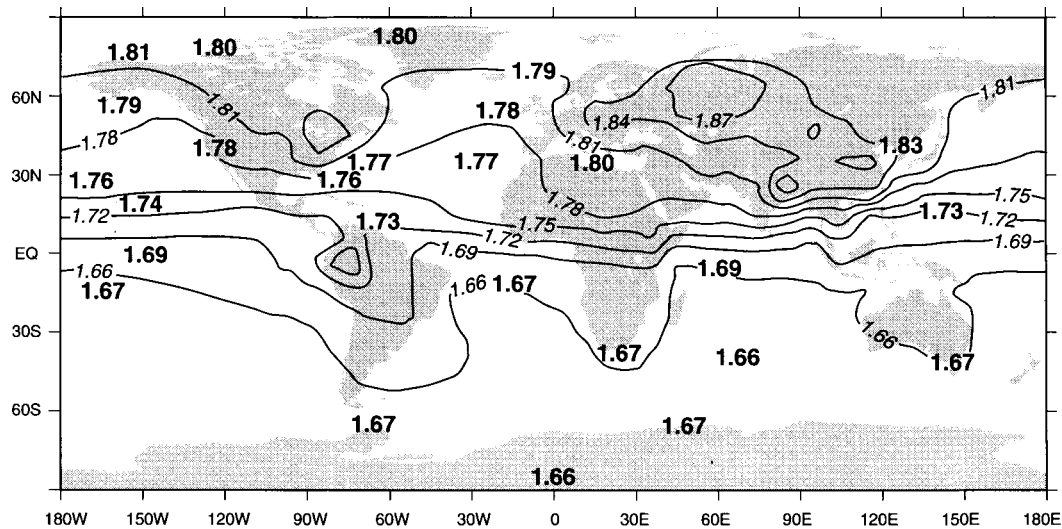


Fig. 3. Model simulated annual mean CH_4 concentrations (isolines) compared to measurements in the year 1992 (bold printed) in $\mu\text{mol/mol}$, derived from the NOAA/CMDL flask sampling network (CDIAC, 1993).

associated with the relatively high northern location of the ITCZ. An annual and global CH_4 maximum occurs over Siberia, caused by the combined influence of European and Asian emissions.

Pre-industrial methane distributions strongly deviate from the current ones, as the total CH_4 source strength has been estimated to be about $265\text{--}270 \text{ Tg yr}^{-1}$ (Table 2). Note that this includes nearly 80 Tg yr^{-1} from mid-19th century anthropogenic emissions, largely from agricultural activities. We calculate that the hemispheric difference in CH_4 burden was only 2%, while the pole-to-pole concentration difference was about 6%. Analyses of ice cores in Antarctica and Greenland have shown that pre-industrial methane levels near the surface were about $0.7\text{--}0.8 \mu\text{mol/mol}$ (Etheridge et al., 1988), consistent with our simulations of the 1850 scenario (Fig. 4). This provides indirect support for our estimate of the total natural CH_4 source, assuming that it did not undergo major changes during the past century.

In our future-scenario simulations we assume a 65% anthropogenic CH_4 emission growth between 1992 and 2050 (Table 2). We calculate that the global mean CH_4 surface concentration increases further, by about 50%, from 1.72 to $2.55 \mu\text{mol/mol}$, which is a factor of 3–4 higher compared to pre-industrial concentrations (Fig. 4). Our estimate of

the future CH_4 level is 10% lower compared to that of IPCC (1996), which presents a mean CH_4 level of $2.79 \mu\text{mol/mol}$ for the atmosphere in 2050 according to the IS92a scenario. This discrepancy can be explained by the IPCC (1996) assumption that the OH-feedback on the CH_4 lifetime between 1850 and 1992 remains the same between 1992 and 2050, whereas we calculate that this feedback reduces substantially in the future period (Subsection 4.4). As in the 1992 atmosphere, the CH_4 seasonality is to a large extent determined by chemical destruction. Methane emissions are dominated by anthropogenic sources which are relatively constant throughout the year; natural emissions are at maximum during summer when the CH_4 levels reach a minimum.

4.4. Changing CH_4 lifetime

The “lifetime” of methane in the atmosphere is usually defined as the quotient of the CH_4 burden in the atmosphere (4600 Tg in the reference year 1992) and the annual CH_4 breakdown by its reaction with OH and minor loss processes in the stratosphere and in soils (600 Tg yr^{-1} minus annual increase). The model calculated CH_4 lifetime is $4600/580 = 7.9$ years, somewhat less compared to the IPCC (1996) estimate of 8.6 years. Note that IPCC (1996) additionally uses the “turn-

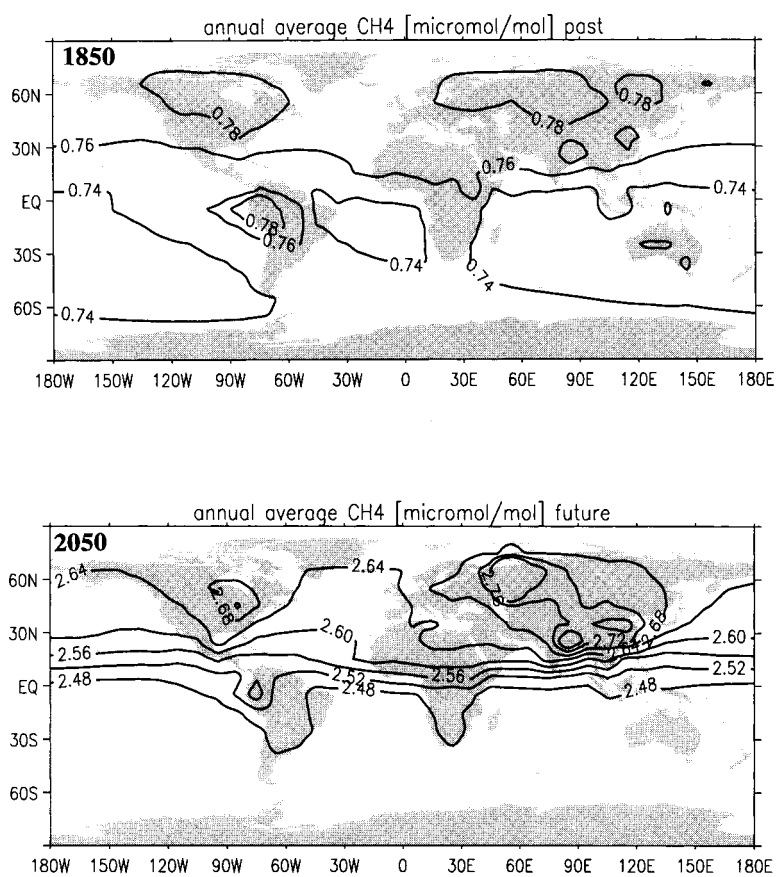


Fig. 4. Model calculated annual mean surface level CH₄ for the past (1850) and future (2050) emission scenarios, in $\mu\text{mol/mol}$.

over time" for "lifetime". Further, IPCC (1994) has applied the concept of "adjustment time" (or response time) to quantify the decay of an instantaneous CH₄ pulse into the atmosphere. The CH₄ adjustment time has been introduced as part of "global warming potential" calculations (Section 5), which are based on emission pulse simulations. The adjustment time of an emission pulse exceeds the lifetime (Prather, 1994). A single CH₄ pulse depletes OH and thus increases the CH₄ lifetime, which is an important positive feedback. Unfortunately, the terms "adjustment time", "turnover time" and "lifetime" are quite confusing. For example, the IPCC (1996) Summary for Policymakers mentions a lifetime of 12 ± 3 years although this refers to the adjustment time.

Previous studies have demonstrated that global

OH levels are dependent on simultaneous emissions of tropospheric O₃ precursors, mainly CH₄, CO and NO_x (Thompson and Cicerone, 1986; Isaksen and Hov, 1987; Crutzen and Zimmermann, 1991). The relevant chemical feedbacks and controlling processes have been summarized in Subsection 4.1. Although photodissociation of O₃ in the presence of water vapour (R1-2) is the dominant hydroxyl source, the partitioning between OH and HO₂ is strongly affected by the reactions CO+OH and NO+HO₂. Further, the reaction with CO is a major direct OH sink. Nonetheless, CH₄ oxidation by OH contributes to CO formation so that CO and CH₄ emissions are global hydroxyl sinks of similar magnitude.

Fig. 5 shows the calculated annual and zonal

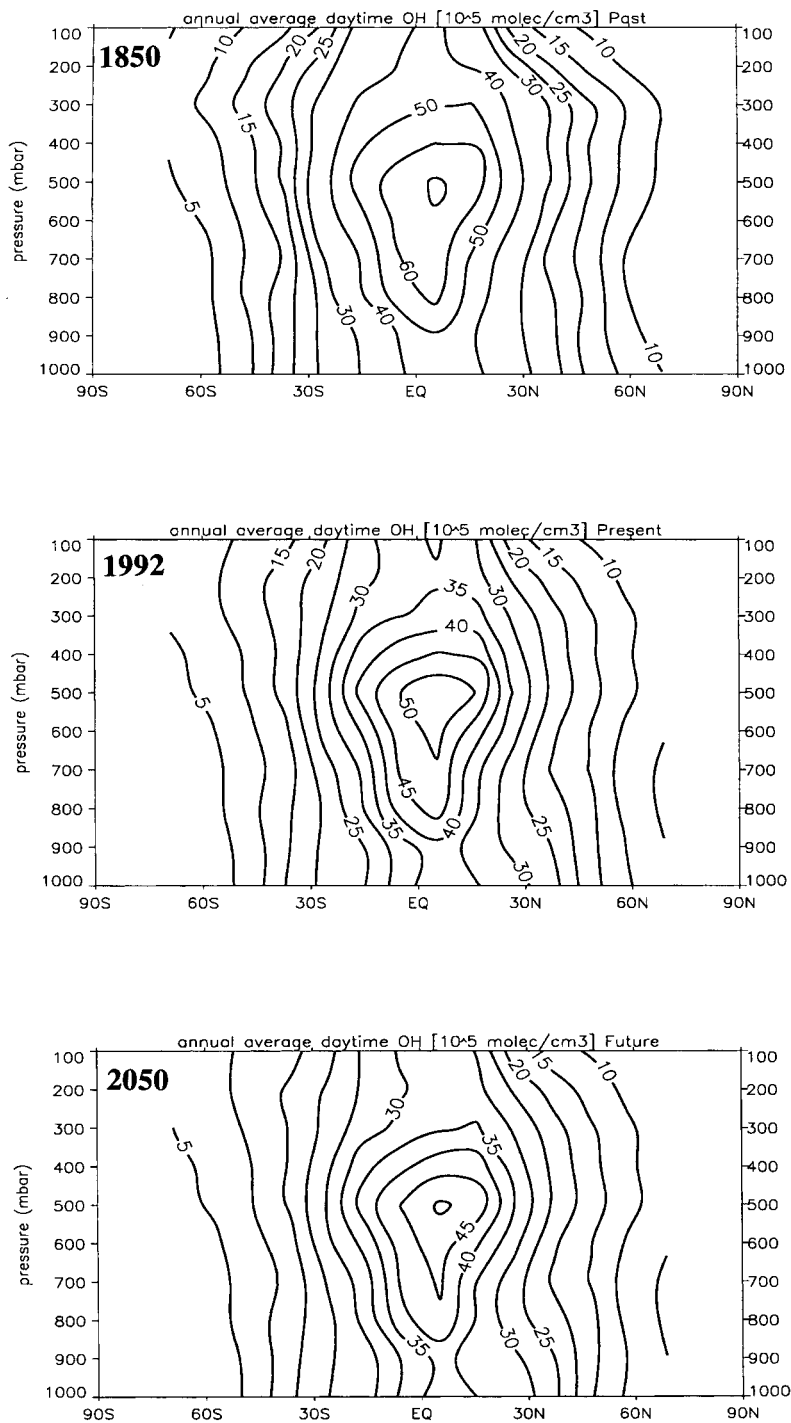


Fig. 5. Model calculated annual and zonal mean, daytime OH levels for the past (1850), present (1992) and future (2050) emission scenarios, in molecules cm^{-3} .

mean OH distributions for the past, current and future emission scenarios. Relatively small OH changes occur in high latitudes, in particular in the southern hemisphere. However, we calculate that in middle latitudes in the northern hemisphere and in the tropics significant OH reductions have taken place between 1850 and 1992. It seems likely that the major part of these OH reductions, particularly in the extratropics, have occurred before 1980. After this period stratospheric O₃ depletion has enhanced tropospheric OH formation. It appears that most of the 1850–1992 OH changes have occurred over the oceans. Relatively minor hydroxyl changes occurred over the continents in industrialized and biomass burning areas where enhanced O₃ levels and, consequently, OH formation compensate OH depletion by increasing CH₄ and CO. Comparing the 1850 and 1992 simulations shows that in the NO_x-poor marine environments increasing CH₄ and CO reduce OH. Fig. 5 also illustrates that the OH change between 1850 and 1992 is comparatively larger than that during the 1992–2050 period.

In the 2050 simulation the most significant NO_x and thus O₃ increases occur over southern Asia and central America. In general, increasing NO_x emissions by countries with emerging economies and associated pollution problems reduce the tropospheric volume of NO_x-poor air, thus enhancing large-scale O₃ and OH formation. Consequently, the fraction of the troposphere in which oxidation of CH₄ and CO depletes OH reduces significantly. This effect of increasing NO_x in the future simulation is most pronounced in the tropics where strong industrial and traffic emission increases are expected. Currently, tropical emissions are dominated by biomass burning, being less efficient in producing NO_x compared to fossil fuel combustion. The overall effect is that the background NO_x-poor tropical troposphere will be increasingly converted into an NO_x-rich environment. This partly counteracts the hydroxyl depletion caused by increasing CH₄ and CO emissions. In summary, our simulations show that during industrialization atmospheric OH has reduced substantially, particularly in the tropics, so that the lifetime of CH₄ has increased from 6.2 years in 1850 to 7.9 years in 1992. However, during the next decades the CH₄ lifetime may not increase proportionally, increasing only by about 6% to

8.4 years in 2050, despite the anticipated strong growth of CH₄ and CO emissions (Table 9).

5. Climate forcing and indirect effects

The actual greenhouse effect of one molecule of CH₄ in the atmosphere is about 25 times that of CO₂. On the other hand, the absolute increase of CO₂ is 200 times larger. The radiative forcings from increasing greenhouse gases (GHG) are defined as the consequent changes in outgoing infrared irradiance (=radiant flux density in W m⁻²) at the top of the atmosphere. Since stratospheric temperatures respond relatively quickly to GHG changes (within months) these are allowed to adjust to the forcing (radiative equilibrium). Because the rest of the climate system adjusts much more slowly (within decades), the tropospheric temperatures are kept fixed in the calculations and we calculate the effect on the outgoing infrared radiation (WMO, 1992). The radiative forcing calculations for methane must account for spectral overlap with nitrous oxide. For the N₂O level in 2050 we adopt 370 nmol/mol (IPCC, 1996), in addition to the 1850 and 1992 levels given in Table 2.

Our calculations show that the radiative forcing from increasing CH₄ between 1850 and 1992 is 0.44 W m⁻², slightly less than the 0.47 W m⁻² presented by IPCC (1996). This CH₄ forcing of 0.44 W m⁻² is about 28% of that by CO₂ (1.6 W m⁻²) and about 18% of the cumulative forcing by all well-mixed greenhouse gases (2.47 W m⁻²) i.e., by increasing CO₂, CH₄, N₂O and CFCs. Furthermore, we calculate that the additional future CH₄ radiative forcing based on the 2050 emission scenario is 0.28 W m⁻² (Table 10), based on a global mean CH₄ level of 2.55 μmol/mol (Subsection 4.3). This would be

Table 9. *Calculated CH₄ lifetime in the past (1850), current (1992) and future (2050) atmosphere*

Year	Lifetime (yr)
1850	6.2
1992	7.9
2050	8.4

Table 10. Calculated CH_4 radiative forcings and indirect effects (W/m^2); the contribution by decreasing OH is indicated between parentheses

	1850–1992	1992–2050
direct effect (including OH feedback)	0.44 (0.11)	0.28 (0.01)
indirect effects		
tropospheric ozone	0.11	0.07
stratospheric H_2O	0.02	0.01
total CH_4	0.57	0.36
forcing by CO_2	1.6	2.3
CH_4 relative to CO_2	35%	15%

about 12% of that by CO_2 (2.3 W m^{-2} , assuming a CO_2 level of $510 \mu\text{mol}/\text{mol}$ in 2050).

It also follows that the radiative forcing per CH_4 increment becomes smaller as the atmospheric CH_4 burden increases, due to saturation of the CH_4 spectral lines (most importantly in the $7.6 \mu\text{m}$ band). For the past CH_4 trend (1850–1992) we obtain a mean radiative forcing of 0.46 W m^{-2} per $\mu\text{mol}/\text{mol}$ CH_4 increase, while in future (1992–2050) this reduces by about 25% to 0.34 W m^{-2} per $\mu\text{mol}/\text{mol}$ CH_4 that is added to the atmosphere. In fact, the radiative effects of both CH_4 and CO_2 are non-linearly dependent on their concentration. Nevertheless, the factor of 25 difference in “greenhouse effectiveness” of these molecules remains approximately constant on the century time scale that is considered here.

In addition to the direct radiative forcing, indirect chemical effects also contribute through formation of radiatively active gases, notably tropospheric O_3 and stratospheric water vapour. This increases the direct effect by approximately 30% (Lelieveld et al., 1993; IPCC, 1994). The major part of this is due to tropospheric O_3 formation (Table 10), while the stratospheric H_2O effect contributes only about 5%. Altogether, increasing tropospheric O_3 from man-made CH_4 , CO and NO_x emissions contributes 0.38 W m^{-2} to the 1850–1992 global mean radiative forcing, while for the 1992–2050 scenario this adds 0.28 W m^{-2} , equal to the direct forcing by increasing CH_4 (Van Dorland et al., 1997).

We have performed sensitivity calculations by individually increasing NO_x , CO and CH_4 emissions from the 1850 to 1992 levels. Thus we derive that the contribution of anthropogenic CH_4 emis-

sions to increasing tropospheric O_3 is roughly equal to that by CO emissions (both about one quarter), while the other half should be attributed to NO_x emissions. Furthermore, increasing CH_4 also alters the chemistry of stratospheric O_3 , however, the effect on climate is only minor. It should be noted that the CH_4 -OH positive feedback on the methane lifetime (i.e., more CH_4 → less OH → more CH_4) also contributes to the climate effect, which is included in the CH_4 radiative forcing calculations presented above. We calculate that this feedback added about 25% to the direct CH_4 effect between 1850 and 1992, while it contributes only about 5% in the future scenario (Table 10). Fig. 6 shows the contribution of CH_4 to climate forcing relative to the other GHGs for the 1850–1992 period. Further, our calculations suggest that the contribution by CH_4 relative to that of CO_2 will decrease substantially, from 35% in 1992 to 15% in 2050 (Table 10).

To compare the cumulative climate perturbations of different greenhouse gases in time, “relative radiative forcings” are applied (Rodhe, 1990). The most commonly used index of radiative forcing is the global warming potential (GWP). The GWP of methane is the time integrated radiative forcing from the release of 1 kg of CH_4 relative to that of 1 kg of CO_2 (IPCC, 1990)*. The time integration implies that the trace gas lifetimes as well as their climate forcings are explicitly considered. Thus, the model calculated GWP describes how much stronger a just emitted amount of CH_4 perturbs the atmospheric radiation balance over a 20–500 year period (typically 100 years) compared to a simultaneously emitted amount of CO_2 . The lifetime of CO_2 (50–200 years) is determined by relatively rapid dissolution in the upper layer of the oceans (within several years) and century time scale exchange processes with the deep oceans. The IPCC recommended GWP integration time intervals are 20, 100 and 500 years. The GWP of methane decreases as longer time integrations are applied (> 10 years), since the CO_2

* A GWP can be expressed in kg/kg, referring to the units commonly used for emissions, or in mol/mol, referring to the comparison of a molecule of CH_4 with a molecule of CO_2 . The mass units can be converted into molar units by dividing by $M_{\text{CO}_2}/M_{\text{CH}_4} = 2.75$, the ratio of the CO_2 and CH_4 molecular weights.

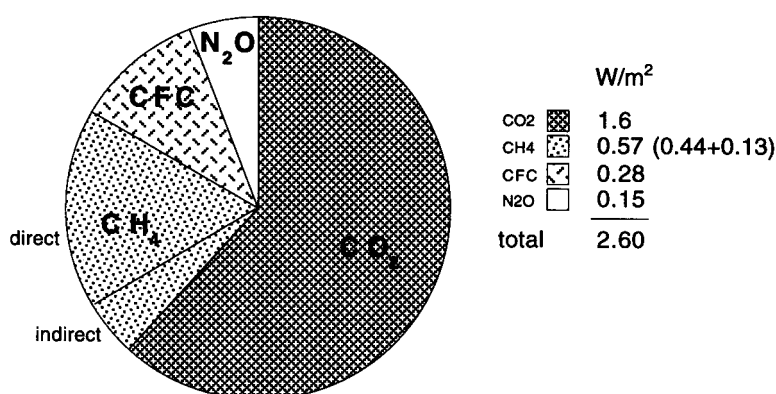


Fig. 6. Calculated contributions of the long-lived greenhouse gases to radiative forcing of climate during the period 1850–1992. The contribution of methane (0.57 W/m²) includes the direct (0.44 W/m²) and indirect chemical effects (0.13 W m⁻²).

lifetime exceeds that of CH₄ by an order of magnitude.

The GWPs of methane for the three IPCC recommended time horizons are listed in Table 11. The GWP values pertaining to the indirect forcing are also included, i.e., indirect effects from radiatively active CH₄ reaction products. The GWPs that include indirect effects agree closely with those presented by IPCC (1996), although our GWP for 20 years is slightly higher (7%). The relevant time horizon depends on the policy application. For example, the most suitable for the evaluation of long-term climate changes associated with global ocean circulations is 500 years, for sea level change it is 100 years, while for continental and ocean surface warming it is 20 years (IPCC, 1990). The time horizon most commonly used is 100 years because it approximates the lifetime of CO₂, the dominant climate forcing agent. The 100 year time horizon is thus particularly useful in comparing the GWPs of fossil fuel

Table 11. Global warming potentials of CH₄ and indirect chemical effects; the contributions by indirect effects are indicated between parentheses

Time horizon (yr)	GWP ^a
20	60 (18)
100	21 (4)
500	7 (1)

^a Expressed in units of kgCH₄/kgCO₂; conversion into mol/mol by dividing by 2.75.

related emissions (Lelieveld et al., 1993). By this measure the emission of 1 kg CH₄ to the present-day atmosphere is 21 times more effective in perturbing the radiative balance compared to that of 1 kg CO₂. Note that on a molecule/molecule basis this ratio is 7.6.

6. Conclusions

After carbon dioxide, methane is the most important contributor to the radiative forcing of climate, in particular if we include indirect effects brought about by chemical changes in the atmosphere. While about 75% of the anthropogenic CO₂ emissions are caused by the use of fossil fuels, for CH₄ this fraction is roughly 25%. The estimated present-day total CH₄ source is 600 Tg yr⁻¹, of which 110 ± 45 is due to releases from the mining/production, transport, storage, distribution and combustion of coal, oil and gas. The contribution by coal mining is about 45 Tg yr⁻¹ and that by oil and gas use 65 Tg yr⁻¹. There is insufficient information available to unequivocally distinguish between the oil and gas related emissions. Field measurements of CH₄ and its isotopes, and associated modelling, are required to reduce the uncertainties.

Agricultural emissions are an important factor in the atmospheric CH₄ budget, contributing about 230 Tg yr⁻¹ (nearly 40%) to the current total source, i.e., more than half of the anthropogenic CH₄ source. Biomass burning (40 Tg yr⁻¹),

domestic ruminants (80 Tg yr^{-1}), volatilization from animal wastes (30 Tg yr^{-1}) and rice production (80 Tg yr^{-1}) predominate. In addition, domestic wastes and industrial sewage are important CH_4 sources. Currently, only about 30% of the total CH_4 source is natural, and this fraction is expected to reduce to about 20% in the year 2050. Since the current total anthropogenic CH_4 source is about 410 Tg yr^{-1} , a reduction of these emissions by about 5% ($\sim 20 \text{ Tg yr}^{-1}$) would stabilize the atmospheric CH_4 level. It should be possible to achieve this reduction through relatively minor emission control measures, e.g., by applying improved technology in waste treatment, recycling, biogas recovery and energy production.

The strong upward CH_4 trend in the 1970s and early 1980s declined by about a factor of 2 to $8\text{--}9 \text{ nmol/mol yr}^{-1}$ in the late 1980s and early 1990s. We performed a sensitivity study based on observed stratospheric O_3 loss between 1980 and 1990, indicating a CH_4 trend reduction of about 1 nmol/mol per decade due to increases of tropospheric UV penetration and OH formation. We conclude that the decelerating CH_4 growth rate during the past decade can only partly be explained by atmospheric chemical effects. Consequently, reduction of the global source strength was probably an important factor.

An enhanced temporary decline of the CH_4 trend occurred in 1992, being strongest in the tropical and sub-tropical northern hemisphere. We infer that this was at least partly due to temperature and associated hydrological effects caused by the Mt Pinatubo sulfate cloud in the stratosphere. The temporary cooling at the surface and reduced precipitation during the summer monsoon in 1992 affected the CH_4 emissions from natural wetlands and rice fields. For example, the emissions from rainfed rice fields in southern Asia, where the temperature sensitivity of methanogenesis is at maximum, may have decreased significantly during this period. Additional temporary factors were the Pinatubo aerosol induced tropospheric UV and OH enhancement and a reduction of biomass burning emissions.

We performed emission scenario calculations for the years 1850, 1992 and 2050 (IPCC-IS92a). The simulated CH_4 distributions for 1992 agree well with observations, and the calculated pre-industrial CH_4 levels are consistent with informa-

tion from ice cores. We calculate that the lifetime of CH_4 in the atmosphere increased from 6.2 to 7.9 years during the 1850–1992 period, resulting from OH depletion by CH_4 and CO emissions. Future anthropogenic emissions can further reduce OH and thus increase the CH_4 lifetime. However, this effect will be moderated by the expected large scale NO_x and O_3 pollution from emissions in tropical and subtropical countries, associated with their emerging economies. On the basis of our future scenario we derive a CH_4 lifetime of 8.4 years in the year 2050.

The calculated 1850–1992 direct radiative forcing of climate by increasing CH_4 is 0.44 W m^{-2} , and for the 1992–2050 period we obtain 0.28 W m^{-2} . The contribution of increasing O_3 in the troposphere to the radiative forcing of climate is similar to that of CH_4 . About one quarter of this O_3 effect is attributed to CH_4 oxidation in the atmosphere, a main indirect effect. Other indirect effects, i.e., by the CH_4 reaction products CO_2 and H_2O (the latter is only relevant in the stratosphere) are minor, adding only about 5% to the direct effect. In fact, the CO_2 effect is negligible because most of it ($\sim 80\%$) derives from biogenic CH_4 so that it is recycled CO_2 . The indirect effects enhance the direct CH_4 forcing for 1850–1992 from 0.44 to 0.57 W m^{-2} ; the calculated CH_4 forcing (direct and indirect) for 1992–2050 is 0.36 W m^{-2} . The calculated 1992 radiative forcing by CH_4 (direct and indirect) is 35% of that by CO_2 ; we expect that this will reduce to about 15% by the middle of the next century.

The calculated GWPs of CH_4 over 20, 100 and 500 year time horizons are 60, 21 and 7, respectively (mass CH_4/CO_2). Thus the relative climate influence of anthropogenic CH_4 emissions compared to those of CO_2 is largest when evaluated over a time horizon of decades but it diminishes on a time scale of centuries. The century time scale is recommended, since it most closely approximates the lifetime of CO_2 , being the most important anthropogenic greenhouse gas.

7. Acknowledgements

We thank Rob van Dorland (KNMI) for his help with the radiative transfer calculations and

Ruhrgas A. G. (Essen) for collaborations and advice about natural gas related methane emissions. This work contributes to the European Union project SINDICATE (Study of the Indirect and Direct Influences on Climate through Anthropogenic Trace-gas Emissions).

REFERENCES

- Andreae, M. O. and Warneck, P. 1994. Global methane emissions from biomass burning and comparison with other sources. *Pure Appl. Chem.* **66**, 162–169.
- Andronova, N. G. and Karol, I. L. 1993. The contribution of USSR sources to global methane emission. *Chemosphere* **26**, 111–126.
- Aselmann, I. and Crutzen, P. J. 1989. Global distribution of natural freshwater wetlands and rice paddies, and their net primary productivity, seasonality and possible methane emissions. *J. Atmos. Chem.* **8**, 307–358.
- Bartlett, K. B. and Harriss, R. C. 1993. Review and assessment of methane emissions from wetlands. *Chemosphere* **26**, 261–320.
- Bekki, S., Law, K. S. and Pyle, J. A. 1994. Effects of ozone depletion on atmospheric CH₄ and CO concentrations. *Nature* **371**, 595–597.
- Berges, M. and Crutzen, P. J. 1996. Estimates of global N₂O emissions from cattle, pig and chicken manure, including a discussion of CH₄ emissions. *J. Atmos. Chem.* **24**, 241–269.
- Bingemer, H. G. and Crutzen, P. J. 1987. The production of methane from solid wastes. *J. Geophys. Res.* **92**, 2181–2187.
- Blake, D. R. and Rowland, F. S. 1988. Continuing worldwide increase in tropospheric methane 1978–1987. *Science* **239**, 1129–1131.
- Born, M., Dörr, H. and Levin, I. 1990. Methane consumption in aerated soils of the temperate zone. *Tellus* **42B**, 2–8.
- Brasseur, G. P. and Granier, C. 1992. Mount Pinatubo aerosols, chlorofluorocarbons, and ozone depletion. *Science* **257**, 1239–1242.
- Carbon Dioxide Information Analysis Center (CDIAC) 1993. *Trends '93. A compendium of data on global change*. World Data Center, Oak Ridge National Laboratory, Oak Ridge, TE.
- Chameides, W. L., Liu, S. C. and Cicerone, R. J. 1977. Possible variations in atmospheric methane. *J. Geophys. Res.* **82**, 1795–1798.
- Chappellaz, J., Barnola, J. M., Raynaud, D., Korotkevich, Y. S. and Lorius, C. 1990. Ice core record of atmospheric methane over the past 160 000 years. *Nature* **345**, 127–131.
- Cicerone, R. J. and Oremland, R. S. 1988. Biogeochemical aspects of atmospheric methane. *Glob. Biogeochem. Cycles* **2**, 299–327.
- Crutzen, P. J. 1995. The role of methane in atmospheric chemistry and climate. In: *Ruminant physiology: digestion, metabolism, growth and reproduction* (edited by W. von Engelhardt et al.). Ferdinand Enke Verlag, Berlin, 291–315.
- Crutzen, P. J., Aselmann, I. and Seiler, W. 1986. Methane production of domestic animals, wild ruminants, other herbivorous fauna, and humans. *Tellus* **38B**, 271–284.
- Crutzen, P. J. and Andreae, M. O. 1990. Biomass burning in the tropics: impact on atmospheric chemistry and biogeochemical cycles. *Science* **250**, 1169–1178.
- Crutzen, P. J. and Zimmermann, P. H. 1991. The changing chemistry of the troposphere. *Tellus* **43A/B**, 136–151.
- Cunnold, D. M., Weiss, R. F., Prinn, R. G., Hartley, D., Simmonds, P. G., Fraser, P. J., Miller, B., Alyea, F. N. and Porter, L. 1997. GAGE/AGAGE measurements indicating reductions in global emissions in CCl₃F and CCl₂F₂ in 1992–1994. *J. Geophys. Res.* **102**, 1259–1269.
- Darmstadter, J., Ayres, L. W., Yares, R. U., Clark, W. C., Crosson, R. P., Crutzen, P. J., Graedel, T. E., McGill, R., Richards, J. F. and Torr, J. A. 1987. *Impacts of world development on selected characteristics of the atmosphere. An integrated approach*. Oak Ridge National Laboratory. ORNL/86–22033/1/V2, Oak Ridge, TE.
- Dentener, F. D. 1993. *Heterogeneous chemistry in the troposphere*. PhD Thesis. Utrecht University.
- Dentener, F. D. and Crutzen, P. J. 1993. Reaction of N₂O₅ on tropospheric aerosols: impact on the global distributions of NO_x, O₃ and OH. *J. Geophys. Res.* **98**, 7149–7163.
- Dlugokencky, E. J., Masarie, K. A., Lang, P. M., Tans, P. P., Steele, L. P. and Nisbet, E. G. 1994a. A dramatic decrease in the growth rate of atmospheric methane in the northern hemisphere during 1992. *Geophys. Res. Lett.* **21**, 45–48.
- Dlugokencky, E. J., Steele, L. P., Lang, P. M. and Masarie, K. A. 1994b. The growth rate and distribution of atmospheric methane. *J. Geophys. Res.* **99**, 17 021–17 043.
- Dlugokencky, E. J., Dutton, E. G., Novelli, P. C., Tans, P. P., Masarie, K. A., Lantz, K. O. and Madronich, S. 1996. Changes in CH₄ and CO growth rates after the eruption of Mt. Pinatubo and their link with changes in tropical tropospheric UV flux. *Geophys. Res. Lett.* **23**, 2761–2764.
- Dutton, J. G. and Christy, J. R. 1992. Solar radiative forcing at selected locations and evidence for global lower tropospheric cooling following the eruptions of El Chichon and Pinatubo. *Geophys. Res. Lett.* **19**, 2313–2316.
- Environmental Protection Agency (EPA) 1993. *Current and future emissions from natural sources* (edited by K. B. Hogan). EPA 430-R-93–011, Washington, DC.
- Environmental Protection Agency (EPA) 1994. *Internation-*

- tional anthropogenic methane emissions: estimates for 1990* (edited by M. J. Adler). EPA 230-R-94-010, Washington, DC.
- Environmental Protection Agency (EPA) 1996. *Methane emissions from the natural gas industry*. EPA 600/R-96-080a, Research Triangle Park, NC.
- Etheridge, D. M., Pearman, G. I. and De Silva, F. 1988. Atmospheric trace gas variations as revealed by air trapped in an ice core from Law Dome, Antarctica. *Ann. Glaciol.* **10**, 28–33.
- Etheridge, D. M., Pearman, G. I. and Fraser, P. J. 1992. Changes in tropospheric methane between 1841 and 1978 from a high accumulation-rate Antarctic ice core. *Tellus* **44B**, 282–294.
- Feichter, J. and Crutzen, P. J. 1990. Parameterisation of deep cumulus convection in a global tracer transport model and its evaluation with ²²²Rn. *Tellus* **42B**, 100–117.
- Food and Agricultural Organization (FAO) 1991. *Production yearbook* United Nations, Rome.
- Fuglestedt, J. S., Jonson, J. E. and Isaksen, I. S. A. 1994. Effect of reductions in stratospheric ozone on tropospheric chemistry through changes in photolysis rates. *Tellus* **46B**, 172–192.
- Fung, I., John, J., Lerner, J., Matthews, E., Prather, M., Steele, L. P. and Frazer, P. J. 1991. Three-dimensional model synthesis of the global methane cycle. *J. Geophys. Res.* **99**, 13 033–13 065.
- Gleason, J. F., Bartia, P. K., Herman, J. R., McPeters, R., Newman, P., Stolarski, R. S., Flynn, L., Labow, G., Larko, D., Seftor, C., Wellemeier, C., Komhyr, W. D., Miller, A. J. and Planet, W. 1993. Record low ozone in 1992. *Science* **260**, 523–526.
- Granier, C., Müller, J. F., Madronich, S. and Brasseur, G. P. 1996. Possible causes for the 1990–1993 decrease in the global tropospheric CO abundances: a three-dimensional sensitivity study. *Atmos. Environ.* **30**, 1673–1682.
- Hao, W. M., Liu, M. H. and Crutzen, P. J. 1991. Estimates of annual and regional releases of CO₂ and other trace gases to the atmosphere from fires in the tropics based on FAO statistics for the period 1975–1980. In: *Fire in the tropical biota* (edited by J. Goldammer). Springer-Verlag, Berlin, 440–462.
- Harriss, R. C. and Frohling, S. 1992. The sensitivity of methane emissions from northern freshwater wetlands to global change. In: *Global warming and freshwater ecosystems* (edited by P. Firth and S. Fisher). Springer-Verlag, Berlin, 48–67.
- Hein, R., Crutzen, P. J. and Heimann, H. 1997. An inverse modelling approach to investigate the global atmospheric methane cycle. *J. Geophys. Res.*, in press.
- Hogan, K. B. and Harriss, R. C. 1994. Comment on “A dramatic decrease in the growth rate of atmospheric methane in the northern hemisphere during 1992” by E. J. Dlugokencky et al. *Geophys. Res. Lett.* **21**, 2445–2446.
- Intergovernmental Panel on Climate Change (IPCC) 1992. *Climate change. The IPCC scientific assessment* (edited by J. T. Houghton, G. J. Jenkins and J. J. Ephraums). Cambridge University Press, Cambridge, UK.
- Intergovernmental Panel on Climate Change (IPCC) 1992. *Climate change 1992. The supplementary report to the IPCC Scientific Assessment* (edited by J. T. Houghton, B. A. Callander and S. K. Varney). Cambridge University Press, Cambridge, UK.
- Intergovernmental Panel on Climate Change (IPCC) 1994. *Climate change 1994. Radiative forcing of climate change* (edited by J. T. Houghton et al.). Cambridge University Press, Cambridge, UK.
- Intergovernmental Panel on Climate Change (IPCC) 1996. *Climate change 1995. The science of climate change* (edited by J. T. Houghton et al.). Cambridge University Press, Cambridge, UK.
- International Energy Agency (IEA) 1997. *Methane emissions from the oil and gas industry*. IEA Report PH2/7, Washington, DC, USA.
- Isaksen, I. S. A. and Hov, O. 1987. Calculation of trends in the tropospheric concentration of O₃, OH, CO, CH₄ and NO_x. *Tellus* **39B**, 271–285.
- Kirchgesner, D. A., Piccot, S. D. and Winkler, J. D. 1993. Estimate of global methane emissions from coal mines. *Chemosphere* **26**, 453–472.
- Labitzke, K. and McCormick M. P. 1992. Stratospheric temperature increases due to Pinatubo aerosols. *Geophys. Res. Lett.* **19**, 207–210.
- Lacis, A. A. and Mishchenko, M. I. 1995. Climate forcing, climate sensitivity, and climate response: A radiative modelling perspective on atmospheric aerosols. In: *Aerosol forcing of climate* (edited by R. J. Charlson and J. Heintzenberg). John Wiley and Sons, Chichester, 11–42.
- Lamb B. K., McManus, J. B., Shorter, J. H., Kolb, C. E., Mosher, B., Harriss, R. C., Allwine, E., Blaha, D., Howard, T., Guenther, A., Lott, R. A., Siverson, R., Westberg, H. and Zimmerman, P. 1995. Development of atmospheric tracer methods to measure methane emissions from natural gas facilities and urban areas. *Environ. Sci. Technol.* **29**, 1468–1479.
- Law, K. S. and Pyle, J. A. 1993. Modelling the budgets of tropospheric trace gases: (2). CH₄ and CO. *J. Geophys. Res.* **98**, 18 401–18 412.
- Levy, H. 1971. Normal atmosphere: Large radical and formaldehyde concentrations predicted. *Science* **173**, 141–143.
- Lelieveld, J. and Van Dorland, R. 1995. Model simulations of ozone chemistry changes in the troposphere and consequent radiative forcings of climate during industrialization. In: *Atmospheric ozone as a climate gas* (edited by W.-C. Wang and I. S. A. Isaksen). NATO ASI Series. Springer-Verlag, Berlin, 227–258.
- Lelieveld, J., Crutzen, P. J. and Brühl, C. 1993. Climate effects of atmospheric methane. *Chemosphere* **26**, 739–768.
- Lobert, J. M., Scharffe, D. H., Hao, W. M., Kuhlbusch, T. A., Seewen, R., Warneck, P. and Crutzen, P. J. 1991. Experimental evaluation of biomass burning

- emissions: nitrogen and carbon containing compounds. In: *Global biomass burning: atmospheric, climatic and biospheric implications* (edited by J. S. Levine). MIT Press, Cambridge, MA, 289–304.
- Lowe, D. C., Brenninkmeijer, C. A. M., Manning, M. R., Sparks, R. and Wallace, G. 1988. Radiocarbon determination of atmospheric methane at Baring Head, New Zealand. *Nature* **332**, 522–525.
- Lowe, D. C., Brenninkmeijer, C. A. M., Brailsford, G. W., Lassey, K. R. and Gomez, A. J. 1994. Concentration and ^{13}C records of atmospheric methane in New Zealand and Antarctica: evidence for changes in methane sources. *J. Geophys. Res.* **99**, 16913–16925.
- Madronich, S. and Granier, C. 1992. Impact of recent total ozone changes on tropospheric ozone photodissociation, hydroxyl radicals and methane trends. *Geophys. Res. Lett.* **19**, 465–467.
- Manning, M. R., Lowe, D. C., Melhuish, W. H., Sparks, R. J., Wallace, G. and Brenninkmeijer, C. A. M. 1990. The use of radiocarbon measurements in atmospheric studies. *Radiocarbon* **32**, 37–58.
- Marland, G. and Rotty, R. M. 1984. Carbon dioxide emissions from fossil fuels: a procedure for estimation and results for 1950–1982. *Tellus* **36B**, 232–261.
- Masters, C. D., Root, D. H. and Attanasi, E. D. 1991. Resource constraints in petroleum production potential. *Science* **253**, 146–152.
- McCormick, M. P., Thomason, L. W. and Trepte, C. R. 1995. Atmospheric effects of the Mt. Pinatubo eruption. *Nature* **373**, 399–404.
- Mitchell, C. 1993. Methane emissions from the coal and natural gas industries in the UK. *Chemosphere* **26**, 441–446.
- Montzka S. A., Butler, J. H., Myers, R. C., Thompson, T. M., Swanson, T. H., Clarke A. D., Lock, L. T. and Elkins, J. W. 1996. decline in the tropospheric abundance of halogen from halocarbons: implications for stratospheric ozone depletion. *Science* **272**, 1318–1322.
- Morcrette, J. J. 1991. Radiation and cloud radiative properties in the European Centre for Medium-range Weather Forecasting system. *J. Geophys. Res.* **96**, 9121–9132.
- Neue, H. U. and Sass, R. L. 1994. Trace gas emissions from rice fields. In: *Global atmospheric-biospheric chemistry* (edited by R. G. Prinn). Plenum Press, New York, 119–147.
- Novelli, P. C., Maarie, K. A., Tans, P. P. and Lang, P. M. 1994. Recent changes in atmospheric carbon monoxide. *Science* **263**, 1587–1590.
- Oort, A. H. 1983. *Global atmospheric circulation statistics, 1958–1973*. NOAA Professional Paper 14, US Government Printing Office, Washington, DC.
- Plotnikov, V. S., Berman, M. and Angerinos, G. F. 1995. FSU's natural gas liquids business needs investment. *Oil & Gas J.* (March 13), 50–56.
- Prather, M. J. 1994. Lifetimes and eigenstates in atmospheric chemistry. *Geophys. Res. Lett.* **21**, 801–804.
- Prinn, R., Weiss, R., Miller, J., Huang, J., Alyea, F., Cunnold, D., Fraser, P., Hartley, D. and Simmonds, P. 1995. Atmospheric trends and lifetime of trichloroethane and global average hydroxyl radical concentrations based on 1978–1994 ALE/GAGE measurements. *Science* **269**, 187–192.
- Quay, P. D., King, S. L., Stutsman, J., Steele, L. P., Fung, I., Gammon, R. H., Brown, T. A., Farwell, G. W., Grootes, P. M. and Smid, F. H. 1991. Carbon isotopic composition of atmospheric CH_4 : Fossil and biomass burning source strengths. *Glob. Biogeochem. Cycles* **5**, 25–47.
- Rasmussen, R. A. and Khalil, M. A. K. 1984. Atmospheric methane in the recent and ancient atmospheres: concentrations, trends, and interhemispheric gradient. *J. Geophys. Res.* **89**, 11 599–11 605.
- Reeburgh, W. S., Roulet, N. T. and Svensson, B. H. 1994. Terrestrial biosphere-atmosphere exchange in high latitudes. In: *Global atmospheric-biospheric chemistry* (edited by R. G. Prinn). Plenum Press, New York, 165–178.
- Robock, A. and Mao, J. 1995. The volcanic signal in surface temperature observations. *J. Climate* **8**, 1086–1103.
- Rodhe, H. 1990. A comparison of the contributions of various gases to the greenhouse effect. *Science* **248**, 1217–1219.
- Shine, K. P., Briegleb, B. P., Grossman, A. S., Hauglustaine, D., Mao, H., Ramaswamy, V., Schwarzkopf, M. D., Van Dorland, R. and Wang, W.-C. 1995. Radiative forcing due to changes in ozone: a comparison of different codes. In: *Atmospheric ozone as a climate gas* (edited by W.-C. Wang and I. S. A. Isaksen). NATO ASI Series. Springer-Verlag, Berlin, 373–396.
- Shorter, J. H., McManus, J. B., Kolb, C. E., Allwine, E. J., Lamb, B. K., Mosher, B. W., Harriss, R. C., Partch, U., Fischer, H., Harris, G. W., Crutzen, P. J. and Karbach, H.-J. 1996. Methane emission measurements in urban areas in eastern Germany. *J. Atmos. Chem.* **24**, 121–140.
- Steele, L. P., Fraser, P. J., Rasmussen, R. A., Khalil, M. A. K., Crawford, T. J., Gammon, R. H., Masarie, K. A. and Thoning, K. W. 1987. The global distribution of methane in the troposphere. *J. Atmos. Chem.* **5**, 125–171.
- Steele, L. P., Dlugokencky, E. J., Lang, P. M., Tans, P. P., Martin, R. C. and Masarie, K. A. 1992. Slowing down of the global accumulation of atmospheric methane during the 1980s. *Nature* **358**, 313–316.
- Sugawara, S., Nakazawa, T., Inoue, G., Machida, T., Mukai, H., Vinnichenko, N. K. and Khattatov, U. 1996. Aircraft measurements of the stable carbon isotope ratio of atmospheric methane over Siberia. *Global Biogeochem. Cycles* **10**, 223–231.
- Thompson, A. M. and Cicerone, R. J. 1986. Possible perturbations to atmospheric CO , CH_4 and OH . *J. Geophys. Res.* **91**, 10 853–10 864.
- Tohjima Y., Maksyutov, S., Machida, T. and Inoue, G. 1996. Airborne measurements of atmospheric methane over oil fields in western Siberia. *Geophys. Res. Lett.* **23**, 1621–1624.

- Van Dorland, R., Dentener, F. J. and Lelieveld, J. 1997. Radiative forcing due to tropospheric ozone and sulfate aerosol. *J. Geophys. Res.*, in press.
- Wahlen, M., Tanaka, N., Henry, R., Deck, B., Zeglen, J., Vogel, J., Southon, J., Shemesh, A., Fairbanks, R. and Broecker, W. 1989. Carbon-14 in methane sources and in atmospheric methane: the contribution from fossil fuel carbon. *Science* **245**, 286–290.
- Westermann, P. 1993. Temperature regulation of methanogenesis in wetlands. *Chemosphere* **26**, 321–328.
- Whalen, S. C. and Reeburgh, W. S. 1992. Interannual variations in tundra methane emissions: a four-year time series at fixed sites. *Global Biogeochem. Cycles* **6**, 139–159.
- World Resources Institute (WRI) 1990. World Resources 1990–1991. Oxford University Press, Oxford, UK.
- World Meteorological Organization (WMO) 1992. *Scientific assessment of ozone depletion*. Report 25. WMO, Geneva.
- World Meteorological Organization (WMO) 1994. *Scientific assessment of ozone depletion*. Report 37. WMO, Geneva.
- Zimmermann, P. H. 1987. MOGUNTIA, a handy global tracer model. In: *Air pollution modelling and its applications*. Proc. NATO/CCMS, Reidel Publ. Co., Dordrecht, The Netherlands, 593–608.
- Zimmermann, P. H., Feichter, J., Rath, H. K., Crutzen, P. J. and Weiss, W. 1989. A global three-dimensional source-receptor model investigation using ^{85}Kr . *Atmos. Environ.* **23**, 25–35.
- Zittel, W. 1997. *Untersuchung zum Kenntnisstand über Methanemissionen beim Export von Erdgas aus Rußland nach Deutschland*. Ludwig-Bölkow-Systemtechnik GmbH, Daimlerstraße 15, D-85521 Ottobrunn.